Phase diagram of dilute nuclear matter: Unconventional pairing and the BCS-BEC crossover

Martin Stein,[1] Xu-Guang Huang,[2,1] Armen Sedrakian,[1] and John W. Clark[3]

[1]*Institute for Theoretical Physics, J. W. Goethe University, D-60438 Frankfurt am Main, Germany*
[2]*Center for Exploration of Energy and Matter and Physics Department, Indiana University, Bloomington, Indiana 47408, USA*
[3]*Department of Physics, Washington University, St. Louis, Missouri 63130, USA*

We report on a comprehensive study of the phase structure of cold, dilute nuclear matter featuring a $^3S_1$-$^3D_1$ condensate at nonzero isospin asymmetry, within wide ranges of temperatures and densities. We find a rich phase diagram comprising three superfluid phases, namely, a Larkin-Ovchinnikov-Fulde-Ferrell phase, the ordinary BCS phase, and a heterogeneous, phase-separated BCS phase, with associated crossovers from the latter two phases to a homogeneous or phase-separated Bose-Einstein condensate of deuterons. The phase diagram contains two tricritical points (one a Lifshitz point), which may degenerate into a single tetracritical point for some degree of isospin asymmetry.

Introduction. Fermionic BCS superfluids, which form loosely bound Cooper pairs at weak coupling, undergo a transition to the Bose-Einstein condensate (BEC) state of tightly bound bosonic dimers, once the pairing strength increases [1,2]. This behavior has been confirmed in experiments on cold atomic gases, where the interactions can be manipulated via the Feshbach mechanism [3,4]. In isospin-symmetric nuclear matter, the transition from the BCS to the BEC state of the $^3S_1$-$^3D_1$ condensate may occur upon dilution of the system, in which case the asymptotic state is a Bose-Einstein condensate of deuterons [5–12]. Isospin asymmetry, induced by weak interactions in stellar environments and expected in exotic nuclei, disrupts isoscalar neutron-proton (np) pairing, since the mismatch in the Fermi surfaces of protons and neutrons suppresses the pairing correlations [13]. The standard Nozières-Schmitt-Rink theory [2] of the BCS-BEC crossover must also be modified, such that the low-density asymptotic state becomes a gaseous mixture of neutrons and deuterons [14]. The $^3S_1$-$^3D_1$ condensates can be important in a number of physical settings: (i) Low-energy heavy-ion collisions produce large amounts of deuterons in final states as putative fingerprints of *SD* condensation [6]. (ii) Large nuclei may feature spin-aligned np pairs, as evidenced by recent experimental findings [15] on excited states in ^{92}Pd; moreover, exotic nuclei with extended halos provide a locus for n-p Cooper pairing. (iii) Directly relevant to the parameter ranges covered in the present study are the observations that supernova and hot proto-neutron-star matter at subsaturation densities have low temperature and low isospin asymmetry and that the deuteron fluid is a substantial constituent [16,17].

Two relevant energy scales for the problem domain under study are provided by the shift $\delta\mu = (\mu_n - \mu_p)/2$ in the chemical potentials μ_n and μ_p of neutrons and protons from their common value μ_0 and the pairing gap Δ_0 in the $^3S_1$-$^3D_1$ channel at $\delta\mu = 0$. With increasing isospin symmetry, i.e., as $\delta\mu$ increases from zero to values of order Δ_0, a sequence of unconventional phases may emerge. One of these is a neutron-proton condensate whose Cooper pairs have nonzero center-of-mass (CM) momentum [10,18,19]; this phase is the analog of the Larkin-Ovchinnikov-Fulde-

Ferrell (LOFF) phase in electronic superconductors [20,21]. Another possibility is phase separation into superconducting and normal components, proposed in the context of cold atomic gases [22]. At large isospin asymmetry, where $^3S_1$-$^3D_1$ pairing is strongly suppressed, a BCS-BEC crossover may also occur in the isotriplet $^1S_0$ pairing channel, notably in neutron-rich systems and halo nuclei [23–30].

Our main objective is to combine the ideas of unconventional $^3S_1$-$^3D_1$ pairing and the BCS-BEC crossover in a model of isospin-asymmetric nuclear matter and construct a phase diagram for superfluid nuclear matter over wide ranges of density, temperature, and isospin asymmetry, while also including non-BCS pairings. By doing so, we advance the computational treatment of dilute hadronic matter along several lines: (i) The BCS-BEC crossover in isospin-asymmetric systems, studied previously in Ref. [14], is extended to include a phase with broken spatial symmetry and a spatially symmetric but heterogeneous phase. (ii) We extend the earlier studies [10,18,19] of the nuclear LOFF phase to the low-density regime and show that this phase is succeeded by a less dense heterogeneous phase before a transition to the BEC regime occurs. (iii) We provide a treatment of a heterogeneous (phase-separated) neutron-proton condensate in the context of $^3S_1$-$^3D_1$-paired nuclear matter. Finally, we observe that the model explored here belongs to the class of imbalanced fermionic systems that has received wide attention in the contexts of imbalanced ultracold fermionic gases and color superconductivity in dense, cold QCD [31].

Theory. The Green's function of the superfluid, written in the Nambu-Gorkov basis, is given by

$$i\mathscr{G}_{12} = i \begin{pmatrix} G_{12}^+ & F_{12}^- \\ F_{12}^+ & G_{12}^- \end{pmatrix} = \begin{pmatrix} \langle\psi_1\psi_2^+\rangle & \langle\psi_1\psi_2\rangle \\ \langle\psi_1^+\psi_2^+\rangle & \langle\psi_1^+\psi_2\rangle \end{pmatrix}, \quad (1)$$

where $G_{12}^+ \equiv G_{\alpha\beta}^+(x_1, x_2)$, etc., $x = (t, \boldsymbol{r})$ denotes the continuous temporal-spatial variables, and Greek indices label discrete spin and isospin variables. Each operator in Eq. (1) can be viewed as a bispinor, i.e., $\psi_\alpha = (\psi_{n\uparrow}, \psi_{n\downarrow}, \psi_{p\uparrow}, \psi_{p\downarrow})^T$, where the internal variables $\uparrow, \downarrow$ label a particle's spin, and n, p its isospin. The matrix propagator obeys the familiar Dyson

equation, which has the formal solution

$$\left(\mathscr{G}_{0,13}^{-1} - \Xi_{13}\right)\mathscr{G}_{32} = \delta_{12}, \qquad (2)$$

in terms of the matrix self-energy Ξ, where summation and integration over repeated indices is implicit. Equation (2) is advantageously transformed into momentum space, where it becomes an algebraic equation. For our purposes, translational invariance cannot be assumed, so we proceed by defining relative and CM coordinates $\tilde{r} = (x_1 - x_2)$ and $R = (x_1 + x_2)/2$ and Fourier transforming with respect to the relative four-coordinate and CM three-coordinate $\boldsymbol{R}$. The associated relative momentum is denoted below by $k \equiv (ik_\nu, \boldsymbol{k})$ and the three-momentum of the CM is denoted by $\boldsymbol{Q}$. The zero component of the vector k takes discrete values $k_\nu = (2\nu + 1)\pi T$, where $\nu \in \mathbb{Z}$ and T is the temperature. Thus the Fourier image of Eq. (2) is written as

$$\left[\mathscr{G}_0(k, \boldsymbol{Q})^{-1} - \Xi(k, \boldsymbol{Q})\right]\mathscr{G}(k, \boldsymbol{Q}) = \mathbf{1}_{8\times 8}. \qquad (3)$$

The normal propagators for the particles and holes are diagonal in both spaces, i.e., $(G^+, G^-) \propto \delta_{\alpha\alpha'}$; hence the off-diagonal elements of $\mathscr{G}_0^{-1}$ are zero. Writing out the non-vanishing components in the Nambu-Gorkov space explicitly, we obtain $[\mathscr{G}_0(ik_\nu, \boldsymbol{k}, \boldsymbol{Q})^{-1}]_{11} = -[\mathscr{G}_0(-ik_\nu, \boldsymbol{k}, -\boldsymbol{Q})^{-1}]_{22} = G_0^{-1}(ik_\nu, \boldsymbol{k}, \boldsymbol{Q})$, where

$$G_0(k)^{-1} = \text{diag}(ik_\nu - \epsilon_{n\uparrow}^+, ik_\nu - \epsilon_{n\downarrow}^+, ik_\nu - \epsilon_{p\uparrow}^+, ik_\nu - \epsilon_{p\downarrow}^+) \qquad (4)$$

with $\epsilon_{n\uparrow}^\pm = \epsilon_{n\downarrow}^\pm = E_S - \delta\mu \pm E_A$ and $\epsilon_{p\uparrow}^\pm = \epsilon_{p\downarrow}^\pm = E_S + \delta\mu \pm E_A$. Here $E_S = (Q^2/4 + k^2)/2m^* - \bar{\mu}$ and $E_A = \boldsymbol{k} \cdot \boldsymbol{Q}/2m^*$, with $\bar{\mu} \equiv (\mu_n + \mu_p)/2$. The effective mass m^* is defined in the usual fashion in terms of the normal self-energy, bare mass m, and Fermi momentum p_F, i.e., $m/m^* = [1 - (m/p)\partial_p\Xi_{11}|_{p=p_F}]$, with the small mismatch between neutron and proton effective masses being neglected. Keeping this mismatch implies changes $E_{S/A} \rightarrow E_{S/A}(1 \pm \delta_m)$ and $\delta\mu \rightarrow \delta\mu + \mu\delta_m$, where $\delta_m = (m_n^* - m_p^*)/(m_n^* + m_p^*) \ll 1$. In the analysis below, δ_m lies in the range $0 \leqslant |\delta_m| \leqslant 0.06$, the upper bound being attained for largest asymmetries and densities relevant to this study.

The quasiparticle spectra in Eq. (4) are written in a general reference frame moving with the CM momentum $\boldsymbol{Q}$ with respect to a laboratory frame at rest. The spectrum of quasiparticles is seen to be two-fold degenerate; i.e., the SU(4) Wigner symmetry of the unpaired state is broken down to spin SU(2). Note that this symmetry is always approximate, since the phase shifts in the isoscalar and isotriplet S waves differ, such that isosinglet pairing is stronger than isotriplet pairing in bulk nuclear matter.

The nucleon-nucleon scattering data show that the dominant attractive interaction in low-density nuclear matter is the $^3S_1$-$^3D_1$-partial wave, which leads to isoscalar (neutron-proton) spin-triplet pairing. Accordingly, the anomalous propagators have the property $(F_{12}^+, F_{12}^-) \propto (-i\sigma_y) \otimes \tau_x$, where σ_i and τ_i are Pauli matrices in spin and isospin spaces. This implies that, in the quasiparticle approximation, the self-energy Ξ has only off-diagonal elements in the Nambu-Gorkov space. Specifically, $\Xi_{12} = \Xi_{21}^+ = i\Delta_{\alpha\beta}$, with $\Delta_{14} = \Delta_{23} = -\Delta_{32} = -\Delta_{41} \equiv i\Delta$, where Δ is the (scalar) pairing gap in the $^3S_1$-$^3D_1$

channel. Substituting Eq. (4) into Eq. (2), we obtain a set of algebraic equations whose solutions provide the "normal" and anomalous Green's functions

$$G_{n/p}^\pm = \frac{ik_\nu \pm \epsilon_{p/n}^\mp}{(ik_\nu - E_{\mp/\pm}^+)(ik_\nu + E_{\pm/\mp}^-)}, \qquad (5)$$

$$F_{np}^\pm = \frac{-i\Delta}{(ik_\nu - E_\pm^+)(ik_\nu + E_\mp^-)}, \qquad (6)$$

$$F_{pn}^\pm = \frac{i\Delta}{(ik_\nu - E_\mp^+)(ik_\nu + E_\pm^-)}, \qquad (7)$$

the four branches of the quasiparticle spectra being given by

$$E_r^a = \sqrt{E_S^2 + \Delta^2} + r\delta\mu + aE_A, \qquad (8)$$

in which $a, r \in \{+, -\}$. Analytic continuation of these Green's functions via $ik_\nu \rightarrow k_0 + i0^+$ yields their retarded counterparts. The densities of neutrons and protons in any of the superfluid states are obtained through

$$\rho_{n/p}(\boldsymbol{Q}) = -2\int \frac{d^4k}{(2\pi)^4}\text{Im}[G_{n/p}^+(k, \boldsymbol{Q}) - G_{n/p}^-(k, \boldsymbol{Q})]f(\omega), \qquad (9)$$

where $k = (k_0, \boldsymbol{k})$ and $f(x) = 1/[\exp(x/T) + 1]$. In mean-field approximation, the anomalous self-energy (pairing gap) is determined by

$$\Delta(\boldsymbol{k}, \boldsymbol{Q}) = 2i\int \frac{d^4k'}{(2\pi)^4}V(\boldsymbol{k}, \boldsymbol{k}')$$
$$\times \text{Im}[F_{np}^+(k, \boldsymbol{Q}) - F_{pn}^-(k, \boldsymbol{Q})]f(\omega), \qquad (10)$$

where $V(\boldsymbol{k}, \boldsymbol{k}')$ is the neutron-proton interaction potential. Performing a partial-wave expansion in Eq. (10) as well as the integration over k_0, we find

$$\Delta(Q) = \frac{1}{2}\sum_{a,r}\int \frac{d^3k'}{(2\pi)^3}V_{l,l'}(k, k')$$
$$\times \frac{\Delta_{l'}(k', Q)}{2\sqrt{E_S(k')^2 + \Delta_{l'}(k', Q)}}[1 - 2f(E_a^r)], \qquad (11)$$

where $V_{l,l'}(k, k')$ is the interaction in the $^3S_1$-$^3D_1$ partial wave. The magnitude Q of the CM momentum in Eqs. (9) and (11) is a parameter to be determined by minimizing the free energy of the system. For the homogeneous (but possibly translationally noninvariant) cases it suffices to find the minimum of the free energy of the superfluid (S) or unpaired (N) phase,

$$F_S = E_S - TS_S, \quad F_N = E_N - TS_N, \qquad (12)$$

where E is the internal energy (statistical average of the system Hamiltonian) and S denotes the entropy. Stability of the superfluid phase requires $F_S < F_N$. Three possibilities exist for the homogeneous phases: (i) $Q = 0$, $\Delta \neq 0$ (BCS phase), (ii) $Q \neq 0$, $\Delta \neq 0$ (LOFF phase), and $\Delta = 0$, $Q = 0$ (unpaired phase). The free energy of the heterogeneous phase (phase-separation case) is constructed as a linear combination of the superfluid and unpaired energies,

$$\mathscr{F}(x, \alpha) = (1 - x)F_S(\alpha = 0) + xF_N(\alpha \neq 0), \qquad (13)$$

where x is the filling fraction of the unpaired component and $\alpha = (\rho_n - \rho_p)/(\rho_n + \rho_p)$ is the density asymmetry. In the superfluid phase (S) one has $\rho_n^{(S)} = \rho_p^{(S)} = \rho^{(S)}$, whereas in the unpaired phase (N) they are rescaled to new values $\rho_{n/p}^{(N)}$. Thus, the net densities of neutrons/protons per unit volume are given by $\rho_{n/p} = (1-x)\rho^{(S)} + x\rho_{n/p}^{(N)}$.

Results. Equations (9) and (11) were solved self-consistently for a pairing interaction given by the bare nucleon-nucleon interaction in the $^3S_1$-$^3D_1$ partial wave, based on the (phase-shift equivalent) Paris potential [32]. The assumed $^3S_1$-$^3D_1$ partial wave implies Cooper pairing in the $S=1$, $T=0$ spin-isospin channel; $^1S_0$ Cooper pairing in the $S=0$, $T=1$ channel may mix and eventually dominate the $^3S_1$-$^3D_1$ pairing at asymptotically small temperatures ($T \leqslant 0.5$ MeV) and large asymmetries. Use of the bare force in Eq. (11) benchmarks the phase diagram; i.e., it is reproducible with any phase-shift-equivalent interaction. However, some regions of the phase diagram may strongly be affected by polarization of the medium. Studies of polarization in neutron matter exemplify the complexity of this problem: while propagator-based methods predict suppression of the gap, quantum Monte Carlo methods predict gaps closer to the BCS result obtained with the bare force (for a recent assessment, see [33]). Here the nuclear mean field was modeled by a Skyrme density functional. The SkIII [34] and SLy4 [35] parametrizations were tested with nearly identical results.

Our results for the BCS phase and BCS-BEC crossover are consistent with earlier studies: we observe a smooth crossover to an asymptotic state corresponding to a mixture of a deuteron Bose condensate and a gas of excess neutrons. The transition from BCS to BEC is established according the following criteria: (i) The average chemical potential $\bar\mu$ changes its sign from positive to negative values, and (ii) the coherence length of a Cooper pair becomes comparable to the interparticle distance, i.e., $\xi \sim d \sim \rho^{-1/3}$ as conditions change from $\xi \gg d$ to $\xi \ll d$.

The nuclear LOFF phase arises as a result of the energetic advantage of translational symmetry breaking by the condensate, in which pairs acquire a nonzero CM momentum $\mathbf{Q}$. As illustrated in Fig. 1 at $\log_{10}(\rho/\rho_0) = -0.5$, where $\rho_0 = 0.16$ fm^{-3} is the nuclear saturation density, the gap in the LOFF phase at nonzero asymmetries and constant temperature has its maximum at finite Q, which results in a maximum of the condensation energy of the pairs. For large asymmetries the maximum gap occurs for large values of Q. At constant asymmetry, a temperature increase shifts the gap maximum and the free-energy minimum of the LOFF phase toward small Q, and at sufficiently high temperature and small asymmetry the BCS state is favored over the LOFF phase. This behavior is well understood in terms of the phase-space overlap of the Fermi surfaces of neutrons and protons, which (at finite asymmetry) increases with temperature and the momentum Q of the Cooper pairs. Thus, as the temperature increases, we expect a restoration of the BCS phase and of the translational symmetry in the superfluid. Obviously, the same restoration occurs when the isospin asymmetry is small enough.

The superfluid phase with phase separation (PS) has the symmetrical BCS phase as one of its components. The
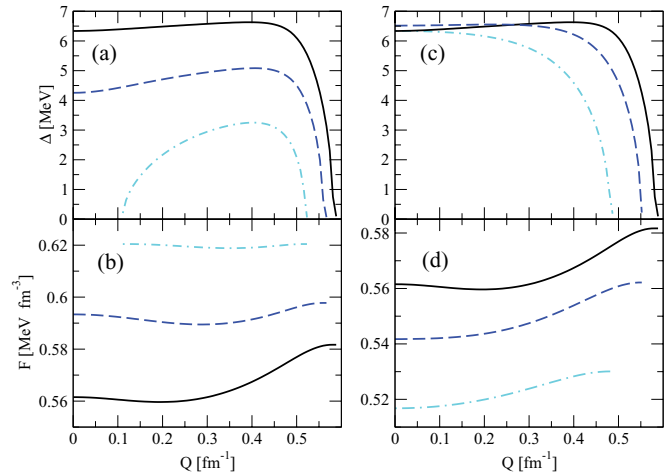

FIG. 1. (Color online) Properties of the nuclear LOFF phase for $\log_{10}(\rho/\rho_0) = -0.5$. Left panel: Dependence of the pairing gap (a) and free energy (b) of the LOFF phase on the total momentum $\mathbf{Q}$ of a Cooper pair at $T = 1$ MeV for asymmetries $\alpha = 0.2$ (solid, black online), 0.3 (dashed, blue online), and 0.4 (dashed-dotted, cyan online). Right panel: Same dependence as in the left panel, but for fixed asymmetry $\alpha = 0.2$ and temperatures of 1 MeV (solid, black line), 2 MeV (dashed, blue online), and 3 MeV (dashed-dotted, cyan online).

temperature dependence of this phase is well established within BCS theory. The second component, which accommodates the neutron excess, is a normal Fermi liquid whose low-temperature thermodynamics is controlled by the excitations in the narrow strip of width $T/\epsilon_{F,n/p}$ around the Fermi surfaces of neutrons and protons.

The transition to the BEC regime of strongly coupled neutron-proton pairs, which are asymptotically identical with deuterons, occurs at low densities. As already well established, in the case of neutron-proton pairing the criteria for the BCS-BEC transition are fulfilled; i.e., $\bar\mu$ changes sign and the mean distance between the pairs becomes larger than the coherence length of the superfluid.

We now turn to the question of how the BCS-BEC crossover is affected by the existence of nuclear LOFF and PS phases at nonzero isospin asymmetries and conversely how these phases evolve in the strongly coupled regime if the density of the system is decreased. The phase diagram of pair-correlated nuclear matter in the density and temperature plane is shown in Fig. 2 for several isospin asymmetries. Four different phases of matter are present in the diagram. (i) The unpaired phase is always the ground state of matter at sufficiently high temperatures $T > T_{c0}$, where $T_{c0}(\rho)$ is the critical temperature of the superfluid phase transition at $\alpha = 0$. (ii) The LOFF phase is the ground state in a narrow temperature-density strip at low temperatures and high densities (marked by LOFF in Fig. 2). (iii) The PS phase appears at low temperatures and low densities. (iv) The isospin-asymmetric BCS phase is the ground state for all densities at intermediate temperatures. In the extreme low-density and strong-coupling regime the BCS superfluid phases have two counterparts: The BCS phase evolves into the BEC phase of deuterons, whereas the PS-BCS phase evolves into the PS-BEC phase, in which
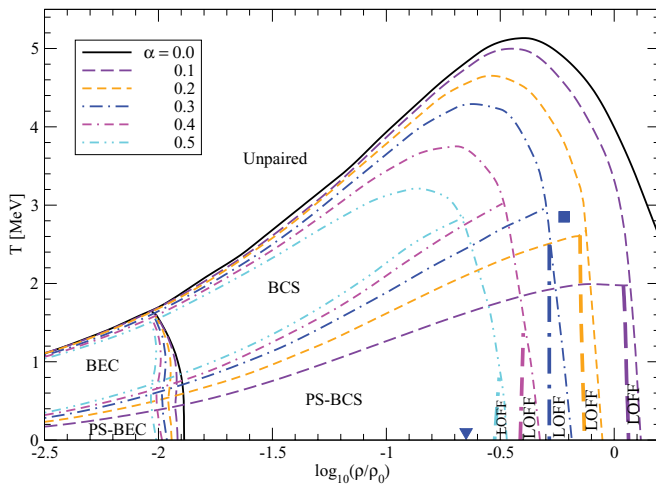
FIG. 2. (Color online) Phase diagram of dilute nuclear matter in the temperature-density plane for isospin asymmetries $\alpha = 0$ (solid, black online), 0.1 (dashed, violet online), 0.2 (short-dashed, orange online), 0.3 (dash-dotted, blue online), 0.4 (double-dash-dotted, magenta online), and 0.5 (dash-double-dotted, cyan online). Included are four phases: unpaired, BCS (BEC), LOFF, and PS-BCS (PS-BEC). For each asymmetry there are two tricritical points, one of which is always a Lifshitz point. For special values of asymmetry these two points degenerate into a single tetracritical point at $\log_{10}(\rho/\rho_0) = -0.22$ and $T = 2.85$ MeV (shown by a square dot) for $\alpha_4 = 0.255$. The LOFF phase disappears at the point $\log_{10}(\rho/\rho_0) = -0.65$ and $T = 0$ (shown by a triangle) for $\alpha = 0.62$. The density-temperature strips where the LOFF phase is the ground state are marked, for each asymmetry, by "LOFF."

the superfluid fraction of matter is a BEC of deuterons. The superfluid-unpaired phase transitions and the phase transitions between the superfluid phases are of second order (thin lines in Fig. 2), with the exception of the PS-BCS to LOFF transition, which is of first order (thick lines in Fig. 2). The BCS-BEC transition and the PS-BCS to PS-BEC transition are smooth crossovers. At nonzero isospin asymmetry the phase diagram features two tricritical points where the simpler pairwise phase coexistence terminates and three different phases coexist. (We do not include the points associated with crossovers from strong to weak coupling in the class of critical points, since

these transitions involve essentially the same phase, i.e., no symmetry is broken).

The topology of the phase diagram and the locations of the tricritical points depend on the value of asymmetry parameter. For $\alpha < \alpha_4$ the low-density critical point corresponds to coexistence of BCS, PS, and LOFF phases, whereas the high-density critical point corresponds to coexistence of LOFF, BCS, and unpaired phases and is thus a Lifshitz point [36]. For $\alpha > \alpha_4$ the topology of the phase diagram changes: The low-density tricritical point contains BCS, PS, and unpaired phases, whereas the high-density tricritical Lifshitz point contains the LOFF-PS–unpaired triple of phases. Clearly, the point with $\log_{10}(\rho/\rho_0) = -0.22$, $T = 2.85$ MeV, and $\alpha_4 = 0.255$ is the special case of a tetracritical point, where all four phases (i.e., BCS, PS, LOFF, and unpaired) coexist.

The extreme low-density region of the phase diagram features two crossovers. At intermediate temperatures we recover the well-known BCS-BEC crossover, where the neutron-proton BCS condensate transforms smoothly into a BEC gas of deuterons with some excess of neutrons. The new ingredient of our phase diagram is the second crossover at low temperatures, where the heterogeneous superfluid phase is replaced by a heterogeneous mixture of a phase containing a deuteron condensate and a phase containing neutron-rich unpaired nuclear matter.

In closing, we note that dilute nuclear matter will definitely feature some clusters of higher mass number, notably ^{3}He, ^{3}H, and ^{4}He, coexisting in statistical equilibrium with the constituents and phases revealed above [16,17]. The α particles (^{4}He) will form a Bose-Einstein condensate at sufficiently low temperatures (see Ref. [37] for a review). These diverse aspects of superfluid, asymmetrical nuclear matter promise significant ramifications for the astrophysics of supernovae and (hot) compact stars and therefore warrant examination in further detail.

[1] A. J. Leggett, in *Modern Trends in the Theory of Condensed Matter*, edited by A. Pękalski and J. A. Przystawa, Vol. 115 of Lecture Notes in Physics (Springer-Verlag, Berlin, 1980), p. 13.

[2] P. Nozières and S. Schmitt-Rink, J. Low Temp. Phys. **59**, 195 (1985).

[3] M. Greiner, C. A. Regal, and D. S. Jin, Nature (London) **426**, 537 (2003).

[4] M. W. Zwierlein, C. A. Stan, C. H. Schunck, S. M. F. Raupach, S. Gupta, Z. Hadzibabic, and W. Ketterle, Phys. Rev. Lett. **91**, 250401 (2003).

[5] T. Alm, B. L. Friman, G. Röpke, and H. Schulz, Nucl. Phys. A **551**, 45 (1993).

[6] M. Baldo, U. Lombardo, and P. Schuck, Phys. Rev. C **52**, 975 (1995).

[7] H. Stein, A. Schnell, T. Alm, and G. Röpke, Z. Phys. A **351**, 295 (1995).

[8] U. Lombardo and P. Schuck, Phys. Rev. C **63**, 038201 (2001).

[9] A. Sedrakian and J. W. Clark, Phys. Rev. C **73**, 035803 (2006).

[10] S. Mao, X. Huang, and P. Zhuang, Phys. Rev. C **79**, 034304 (2009).

[11] X.-G. Huang, Phys. Rev. C **81**, 034007 (2010).

[12] M. Jin, M. Urban, and P. Schuck, Phys. Rev. C **82**, 024911 (2010).

[13] A. Sedrakian and U. Lombardo, Phys. Rev. Lett. **84**, 602 (2000).

[14] U. Lombardo, P. Nozières, P. Schuck, H.-J. Schulze, and A. Sedrakian, Phys. Rev. C **64**, 064314 (2001).

[15] B. Cederwall *et al.*, Nature (London) **469**, 68 (2011).

[16] S. Typel, G. Röpke, T. Klähn, D. Blaschke, and H. H. Wolter, Phys. Rev. C **81**, 015803 (2010).

[17] S. Heckel, P. P. Schneider, and A. Sedrakian, Phys. Rev. C **80**, 015805 (2009).

[18] A. Sedrakian, Phys. Rev. C **63**, 025801 (2001).

[19] H. Müther and A. Sedrakian, Phys. Rev. C **67**, 015802 (2003).

[20] A. I. Larkin and Y. N. Ovchinnikov, Zh. Eksp. Teor. Fiz. **47**, 1136 (1964) [Sov. Phys. JETP **20**, 762 (1965)].

[21] P. Fulde and R. A. Ferrell, Phys. Rev. **135**, 550 (1964).

[22] P. F. Bedaque, H. Caldas, and G. Rupak, Phys. Rev. Lett. **91**, 247002 (2003).

[23] M. Matsuo, Phys. Rev. C **73**, 044309 (2006).

[24] J. Margueron, H. Sagawa, and K. Hagino, Phys. Rev. C **76**, 064316 (2007).

[25] A. A. Isayev, Phys. Rev. C **78**, 014306 (2008).

[26] Y. Kanada-En'yo, N. Hinohara, T. Suhara, and P. Schuck, Phys. Rev. C **79**, 054305 (2009).

[27] T. Abe and R. Seki, Phys. Rev. C **79**, 054002 (2009).

[28] B. Y. Sun, H. Toki, and J. Meng, Phys. Lett. B **683**, 134 (2010).

[29] L. Salasnich, Phys. Rev. C **84**, 067301 (2011).

[30] T. T. Sun, B. Y. Sun, and J. Meng, Phys. Rev. C **86**, 014305 (2012).

[31] A. Sedrakian, J. W. Clark, and M. Alford, *Pairing in Fermionic Systems: Basic Concepts and Modern Applications*, Series on Advances in Quantum Many-Body Theory, Vol. 8 (World Scientific, Singapore, 2006).

[32] J. Haidenbauer and W. Plessas, Phys. Rev. C **30**, 1822 (1984).

[33] S. Gandolfi, A. Y. Illarionov, F. Pederiva, K. E. Schmidt, and S. Fantoni, Phys. Rev. C **80**, 045802 (2009).

[34] R. K. Su, S. D. Yang, and T. T. S. Kuo, Phys. Rev. C **35**, 1539 (1987).

[35] E. Chabanat, P. Bonche, P. Haensel, J. Meyer, and R. Schaeffer, Nucl. Phys. A **635**, 231 (1998).

[36] P. Chaikin and T. Lubensky, *Principles of Condensed Matter Physics* (Cambridge University Press, Cambridge, England, 1995).

[37] T. Yamada, Y. Funaki, H. Horiuchi, G. Röpke, P. Schuck, and A. Tohsaki, in *Clusters in Nuclei, Volume 2*, edited by C. Beck, Vol. 848 of Lecture Notes in Physics (Springer-Verlag, Berlin, 2012), p. 229.